

Nonclassical polarization effects in fluorescence emission spectra from microdroplets

S. Arnold, N. L. Goddard, and S. C. Hill

Citation: *The Journal of Chemical Physics* **111**, 10407 (1999); doi: 10.1063/1.480393

View online: <http://dx.doi.org/10.1063/1.480393>

View Table of Contents: <http://scitation.aip.org/content/aip/journal/jcp/111/23?ver=pdfcov>

Published by the [AIP Publishing](#)

Articles you may be interested in

[Low threshold amplified spontaneous emission from dye-doped DNA biopolymer](#)

J. Appl. Phys. **111**, 113107 (2012); 10.1063/1.4728218

[Polarization induced control of single and two-photon fluorescence](#)

J. Chem. Phys. **132**, 154508 (2010); 10.1063/1.3386574

[Recovery of time evolving fluorescence spectra via sum-frequency cross-correlation frequency resolved optical gating](#)

Appl. Phys. Lett. **87**, 231102 (2005); 10.1063/1.2138366

[Dependence of two-photon-absorption-excited fluorescence on the angle between the linear polarizations of two intersecting beams](#)

Appl. Phys. Lett. **82**, 4642 (2003); 10.1063/1.1585131

[Spontaneous emission spectra from microdroplets](#)

J. Chem. Phys. **108**, 6545 (1998); 10.1063/1.476065



Nonclassical polarization effects in fluorescence emission spectra from microdroplets

S. Arnold^{a)} and N. L. Goddard^{b)}

Microparticle Photophysics Laboratory (MP³L), Polytechnic University, Brooklyn, New York 11201

S. C. Hill

Army Research Laboratory, 2800 Powder Mill Road, Adelphi, Maryland 20783

(Received 23 June 1999; accepted 13 October 1999)

We report a pronounced nonclassical polarization effect on the shape of fluorescence emission spectra from isolated microdroplets containing a dilute solution of soluble fluors or a dilute layer of surfactant fluors. We see different spectral shapes for 90° scattering when comparing between I_{VV} , I_{VH} , I_{HH} , I_{HV} . However, we measure the largest difference in spectral shape in the surfactant case, with the incident polarization directed toward the detector (I_{HV} vs I_{HH}). Imaging reveals that the emission in this case principally arises from two distinct regions near the surface of the droplet, which are diametrically opposed and along the axis of the incident laser beam. The effect appears to be the direct result of coupling between molecular emission moments and electromagnetic modes of the droplet. It is not the molecule which radiates but the molecule microvessel. Directional emission is sensitive to the polarization of the electromagnetic mode which is stimulated by the coupling. © 1999 American Institute of Physics. [S0021-9606(99)70647-1]

We report for the first time, to our knowledge, a system which demonstrates nonclassical behavior in fluorescence polarization experiments. It has been assumed, in fluorescence polarization experiments on single component solutions, that the fluorescence emission spectrum measured at right angles should maintain a constant shape independent of the orientation of the analyzer.¹ However, when solutions are encased in droplets a few microns in size (i.e., several wavelengths) we find that the shape of the emission spectrum is strongly sensitive to the orientation of an analyzer for 90° scattering. We see different spectral shapes when comparing between I_{VV} , I_{VH} , I_{HH} , and I_{HV} . We measure the largest difference in spectral shape in the surfactant case, with the incident polarization directed toward the detector (I_{HV} vs I_{HH}). In this communication we present data for this latter case and show that the effect results from electrodynamic coupling between the molecular emission moment and electromagnetic modes of the droplet. It is not the molecule which radiates but the molecule microvessel.

Spectra were collected from levitated droplets using the setup depicted in Fig. 1. At the heart of the instrument is a standard hyperbolic electrodynamic levitator-trap (SHELT) in which a single particle can be suspended for both spectroscopy and imaging.² The SHELT is sealed within a chamber at 1 atm N₂. The chamber has windows for optical access. Incident light (488 nm) from a linearly polarized Ar⁺ laser is passed through a $\lambda/4$ plate, followed by a Glan Thompson polarizer to alter the polarization to the desired orientation. To reduce photo bleaching the droplet is illuminated for no longer than is needed to take a spectrum by

using a pair of synchronized shutters in front of the laser and the spectrometer CCD. A lens focuses the vertically directed incident beam on the particle (skirt width $\sim 100\ \mu\text{m}$).

The particle is illuminated from below along the $+z$ direction (Fig. 1) and scattering is collected along the x direction. The collection lens system consists of a $f/2.5$ condenser pair, between which is sandwiched a 488 nm notch filter and dichroic analyzing polarizer. The light passed through this condenser is imaged onto a 1/4 m monochromator, with an 1180 G/mm grating and CCD detector (750 \times 242 pixels). The overall resolution of the spectrometer system is 0.08 nm. For imaging, scattered light is collected also along the x axis but from the side opposite the spectrometer. An objective lens (numerical aperture, N.A.=0.4) feeds the light into a standard microscope barrel, where it is filtered and focused onto an imaging CCD camera (192 \times 164 pixels). The overall experimental resolution of the imaging microscope is 0.8 μm .

Samples were prepared using a surfactant carbocyanine dye (D-282) as well as its soluble derivative (H-479) from Molecular Probes, designed as Dil_s(3) and Dil(3), respectively. Bulk samples were prepared and serially diluted so that the final concentration was 10⁻⁶ M in glycerol. To dissolve the surfactant dye into glycerol, a volatile cosolvent, methanol (spectroscopic grade, Aldrich), was added in 2:1 dilution. The cosolvent's purpose is twofold. In addition to enabling dissolution of the dye it reduces the solution's viscosity, so that a micron sized sample can be prepared, charged and injected into the SHELT using a picopipette.³ Following injection into the levitator, the excess methanol quickly evaporates, leaving a droplet with a dilute (~ 1 molecule/1000 nm²) surfactant dye layer on glycerol [Dil_s(3) case], or a uniformly doped glycerol droplet [Dil(3) case].

^{a)}Author to whom correspondence should be addressed. Electronic mail: arnold@photon.poly.edu

^{b)}Present address: Center for Physics and Biology, Rockefeller University, 1230 York Ave., New York, NY 10021.

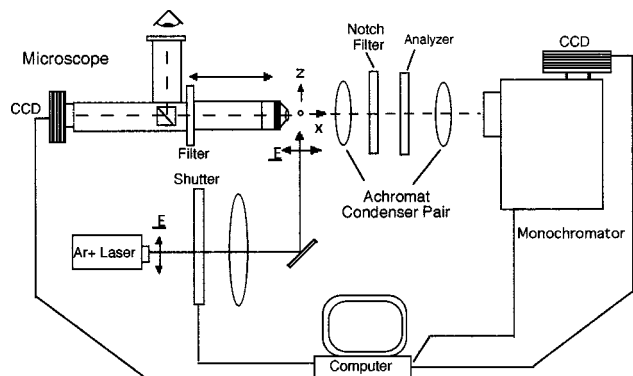


FIG. 1. Basic setup for performing analyzed emission spectra and obtaining images from a single levitated microdroplet.

Although spectra were collected from both bulk and surfactant samples, we present here the surfactant case, where the polarization effects are most distinct. Figure 2 shows a sequence of emission spectra, excited with x polarized light at 488 nm, from a glycerol droplet with 10^{-6} M DiI₃(3). The spectra were taken 32 s apart including the 8 s exposure, in chronological order, Figs. 2(a)–2(c). The spectrum in Fig. 2(a) was taken without an analyzer. The spectra in Figs. 2(b)

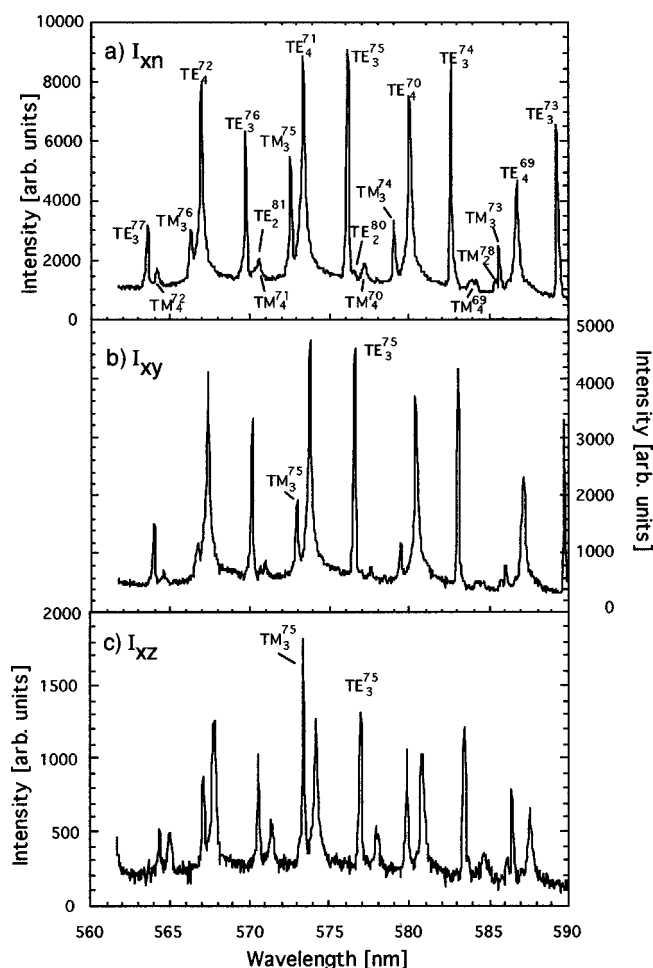


FIG. 2. Fluorescence spectra taken at 90° using x polarized incident radiation with (a) no analyzer, (b) an x oriented analyzer, and (c) a z oriented analyzer.

and 2(c) were taken through the dichroic analyzer oriented along the y and z axes, respectively. The spectra are referred to using the coordinate system in Fig. 1: I_{xN} , I_{xy} , and I_{xz} , correspond to excitation polarized along x with no analyzer (N), analyzer along y , and analyzer along z , respectively. The relationship between our notation and that used conventionally in fluorescence polarization measurements is $I_{xz} = I_{HH}$, $I_{xy} = I_{HV}$.¹ The peaks are due to energy which is coupled from the molecular excited states into electromagnetic modes of the droplet. The modes are designated as P_n^l , where P is the polarization designation (TE for transverse electric, TM for transverse magnetic), l is the angular momentum of the photon in the mode, and n is the mode order.⁴ The modes have been identified in the unanalyzed spectrum by applying a semiclassical model.⁵ The model, which was convolved with the spectrometer's resolution, included demonstrated losses in glycerol,⁶ and produced an excellent fit to the unanalyzed spectrum for a radius of 5.85 μm .

The spectrum in Fig. 2(b) (I_{xy}) is similar to the unanalyzed spectrum in Fig. 2(a) (I_{xN}) although the TM modes are reduced in intensity. The spectrum in Fig. 2(c) (I_{xz}) shows a remarkable difference in shape from that in Fig. 2(b) (I_{xy}). Although transverse electric (TE) modes are highly dominant over transverse magnetic modes (TM) in the I_{xy} spectrum, in the I_{xz} spectrum the TM modes are prominent and in several cases dominate over their TE counterparts (i.e., modes having the same angular momentum and order). For a given pair of modes, we define the enhancement between the z and y analyzed spectra, $E_n^l = [R_n^l]_z / [R_n^l]_y$, in terms of the ratio of intensities $R_n^l = \text{TM}_n^l / \text{TE}_n^l$. Consider the ratio of intensities R_3^{75} : $[R_3^{75}]_y = 0.23$, $[R_3^{75}]_z = 1.5$, and so the enhancement E_3^{75} is greater than six. The same level of enhancement is seen for other mode pairs. Enhancement in TM/TE ratios between z and y analyzer orientations are seen for the soluble dye as well, but to a much smaller extent ($E_n^l < 3$).

Reabsorption can effect mode ratios,^{2,5} but its influence on the data in Fig. 2 can be discounted. Although reabsorption grows as wavelength is decreased, the polarization ratios show no systematic influence of decreasing wavelength. This is not surprising since we have chosen a region of the emission spectrum where longer lived second-order modes, which are normally obscured by reabsorption, are clearly in evidence.

Attempting to understand the difference in shape between the I_{xy} and I_{xz} spectra may seem at first to be difficult since molecules are illuminated at all latitudes and longitudes of the microsphere by a plane wave, and the emission from a given mode into our detector is dependent on the position of the molecule. However, the problem is simplified by imaging the sources of luminescence.

Figure 3 shows an image of a somewhat larger particle (15 μm radius) for x polarized irradiation without an analyzer. This view is what is seen by the slits of our spectrometer. As seen in the topogram to the right, most of the emission arises from two regions of equal intensity diametrically opposed along the z axis. A similar symmetry has been seen in images taken of acceptor luminescence in energy transfer experiments.⁷ It is due to coupling of energy into electromagnetic modes of the particle from the side opposite the

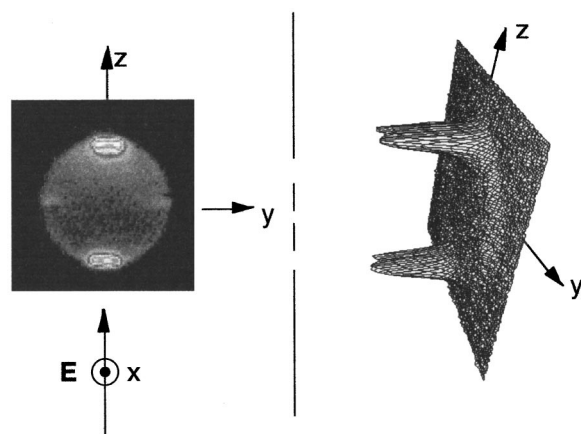


FIG. 3. Image taken at 90° in broad and fluorescence from a Dil(3) doped glycerol droplet $15\ \mu\text{m}$ in radius. The incident light is directed along the z axis and polarized along the x axis.

laser where focusing generates a high probability of excitation. The modes themselves are symmetric in intensity with respect to points diametrically opposed [i.e., $I(\theta, \phi) = I(\pi - \theta, \phi + \pi)$].⁷ The geometrical information supplied from Fig. 2, along with the physics in Ref. 7, suggest that one can reduce the complexity of the physical situation in attempting to understand this fluorescence polarization effect. A further simplification is achieved because Dil_s(3) orients at a glycerol surface with its emission moment tangent to the surface.^{2,5} Our polarization effect can be understood theoretically to first order by positioning emitters on the “pole” just opposite the laser beam (the “top” pole) and orienting their transition moments tangent to the surface (i.e., in the x - y plane).

The Dil_s(3) molecules within the illuminated patch on the surface, near the top pole are photoselected along the x axis with a 2-D (two-dimensional) probability density in proportion to $\cos^2 \phi'$ (the probability of an emitter oriented between ϕ' and $\phi' + d\phi'$ from the x axis is $\cos^2 \phi' d\phi'/\pi$). To gain a rudimentary understanding for our effect we orient an excited molecule in the most probable direction, with its emission moment along x (as shown in Fig. 4), and examine the emission.

An emission peak occurs due to enhanced zero point fluctuations in a photonic mode of the sphere. These fluctuations stimulate the excited molecule to emit into the particular mode. The modes have distinct differences with respect to polarization. Transverse magnetic (TM) modes have local electric fields with both radial and angular components, whereas (TE) modes have only angular components. The mode selected for emission is controlled by frequency and the coupling mechanism. The dipole must be able to project onto the mode (i.e., the Hamiltonian has the form $\hat{p} \cdot \hat{E}$). An x oriented dipole at the top pole easily projects onto TE modes. Analysis of the far field emission from such modes shows that the major component of the radiation pattern in the x - y plane is proportional to $\sin^2(\phi)$, and is y polarized to either side of the x axis; the same as the radiation pattern from a dipole in free space. The explanation for our nonclassical effects lies in the coupling to TM modes.

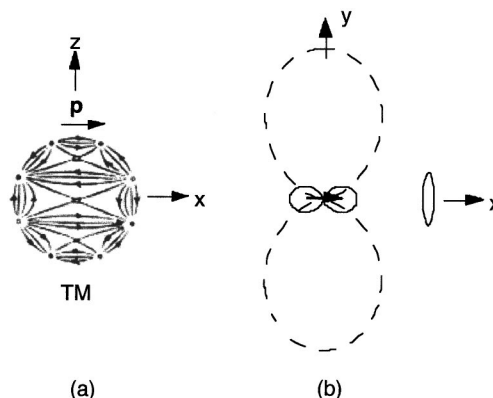


FIG. 4. (a) Pictorial representation of the vector fields in an $l=4$ TM mode (Ref. 8); (b) calculated far field intensity patterns (averaged over a N.A. $=0.2$) in the spectral region of the TM_3^{75} mode (solid) and the TE_3^{75} mode (dashed).

Coupling to TM modes can be understood visually through the original pictorial field diagram offered by Mie for such a mode in 1908.⁸ Figure 4 shows the fields as depicted by Mie for a TM mode having an angular momentum $l=4$.⁸ They are the local fields in the x - z plane. Although they do not display all aspects of the field,⁹ the diagram leads to important insights.

First, the field has both r and θ components. Second, a dipole on the top pole and pointing in the x direction has a finite projection onto such a mode. Without the radial components, Fig. 4(a) represents the far field as well. The emission from such a molecule will be z polarized at 90° (i.e., $\hat{\theta}$ polarized at $\theta=90^\circ$, $\phi=0$) with nodes in θ separated by $\delta\theta=45^\circ$ (more generally $\delta\theta=\pi/l$). Although the θ dependence in the radiation field is similar for both TE and TM modes having common l values, the dependence on the azimuthal angle ϕ as one moves away from the x axis in the x - y plane is quite different. A vector field analysis indicates the θ -component diminishes as $\cos^2 \phi$. Interestingly, both the polarization in the x - y plane and ϕ dependence of the θ -component of radiation field are opposite to our expectations for a free dipole oriented along x ; for a free dipole there would be no intensity emitted along the x axis and the polarization as we move away from the x axis in the x - y plane would be in the y direction. This odd behavior is consistent with the qualitative behavior seen in our spectra. The most pronounced change in spectra shape occurs when we peer in the direction of the excitation polarization (x direction), and the TM contribution to the spectrum is optimized with the analyzer oriented in the z direction [Fig. 2(c)].

The above thoughts, concerning TM modes excited by an x oriented dipole at the top pole, have ignored the fact that a node will appear on the x axis for modes having odd values of l . One can see this by adding two extra nodes to Fig. 3(a) (i.e., to emulate $l=5$). This zero might be expected to have a pronounced effect as one moves from even to odd resonances in a spectrum. However, the spacing between nodes, for our particles ($\delta\theta=\pi/l=\pi/75$) is much smaller than the angular width of our optical detection system [$\Delta\theta=2\sin^{-1}(\text{N.A.})=0.4$]. Consequently the θ dependence of

the emitted intensity is removed by summing of intensities over θ .

The theoretical machinery, for making this discussion more quantitative is at hand.^{10–13} It takes a semiclassical weak coupling approach in which the excited molecule is treated as an oscillating dipole, and solves the electrodynamic boundary value problem for the emitted radiation. We have applied this theory to an x oriented dipole at the top pole. Of particular interest is the ϕ dependence of the emitted radiation within the spectral region of our experiments. Figure 4(b) shows the calculated power collected at the spectral positions of two resonances, TM_3^{75} and TE_3^{75} . The calculations are based on an optical system with our experimental N.A. (0.2), and use a microsphere radius consistent with that determined from the data in Fig. 2 ($5.85\ \mu\text{m}$). The lens is positioned at $\phi=0^\circ$, where it captures a considerable amount of TM radiation. Since this radiation is polarized perpendicular to the figure (z polarized) its relative yield increases for a polarizer oriented in the z direction. The opposite occurs with the lens positioned at $\phi=90^\circ$. The calculated enhancement of the TM/TE ratio between z and y analyzed orientations, E_3^{75} , at $\phi=0^\circ$ is orders of magnitude greater than our measured enhancement of six. This disparity is due in part to analyzing only the x oriented dipole at the top pole. The inclusion of the angular probability density function including all azimuthal molecular orientations, ϕ' , reduces the disparity somewhat, however, the more important limitation is exclusion of other sources which are further from the top pole and clearly in evidence in the image in Fig. 3.

We have shown experimentally that emission from fluorescent molecules within, or at the surface of a spherical microdroplet has nonclassical polarization properties in which the shape of the spectrum depends on the orientation of an analyzer. The effect should be sensitive to the position and orientation of the molecule. This effect is a result of dipole coupling to spherical modes in which the normal di-

pole emission (spatial pattern and polarization properties) is converted to multipole emission. The molecular excited state couples to TM and TE modes having different polarization properties and frequencies.

Our nonclassical polarization effect is the result of the interaction between a spontaneous molecular emission process and a microcavity. It has been shown that spontaneous Raman also displays a rich spectrum associated with microcavity coupling.¹⁴ Consequently we expect a similar nonclassical polarization effect in the Raman case. Raman polarization measurements on levitated droplets were used to infer that the depolarization ratio in a microdroplet is simply a molecular property independent of the spherical boundary.¹⁵ This report is surprising in light of our findings for fluorescence.

We are grateful for support for this research from the National Science Foundation (Grant Nos. ECS 96-34617 and CTS-9625178).

¹ See for example, J. R. Lakowicz, *Principles of Fluorescence Spectroscopy* (Plenum, New York, 1983), Chap. 5.

² S. Arnold, S. Holler, N. L. Goddard, and G. Griffel, *Opt. Lett.* **22**, 1452 (1997).

³ S. Arnold and L. M. Folan, *Rev. Sci. Instrum.* **57**, 2250 (1986).

⁴ S. C. Hill and R. E. Benner, *Morphology-Dependent Resonances*, in *Optical Effects Associated with Small Particles*, edited by P. W. Barber and R. K. Chang (World Scientific, Singapore, 1988), Chap. 1.

⁵ S. Holler, N. L. Goddard, and S. Arnold, *J. Chem. Phys.* **108**, 6545 (1998).

⁶ S. Arnold and L. Folan, *Opt. Lett.* **14**, 387 (1989).

⁷ S. Arnold, S. Holler, and S. D. Druger, *J. Chem. Phys.* **104**, 7741 (1996).

⁸ G. Mie, *Ann. Phys. (N.Y.)* **25**, 377 (1908).

⁹ C. F. Bohren and D. R. Huffman, *Absorption and Scattering of Light by Small Particles* (Wiley, New York, 1983), p. 98.

¹⁰ H. Chew, P. J. McNulty, and M. Kerker, *Phys. Rev. A* **13**, 396 (1976).

¹¹ H. Chew, *J. Chem. Phys.* **87**, 1355 (1987).

¹² S. D. Druger, S. Arnold, and L. M. Folan, *J. Chem. Phys.* **87**, 2649 (1987).

¹³ S. C. Hill, M. D. Barnes, W. B. Whitten, and J. M. Ramsey, *Appl. Opt.* **36**, 4425 (1997).

¹⁴ H.-B. Lin and A. J. Campillo, *Opt. Lett.* **20**, 1589 (1995).

¹⁵ K. H. Fung and I. N. Tang, *Appl. Spectrosc.* **46**, 1189 (1992).